Modal Analysis Investigation of Kris Collision Utilizing Finite Element Method

Waradana, Stesal
Mechanical Engineering, Universitas Sebelas Maret

Ubaidillah
Mechanical Engineering, Universitas Sebelas Maret

Aditya Rio Prabowo
Mechanical Engineering, Universitas Sebelas Maret

Bhre Wangsa Lenggana
Industrial Engineering, Universitas Jenderal Soedirman

他

https://doi.org/10.5109/7236866

出版情報：Evergreen. 11 (3), pp.2234-2247, 2024-09. 九州大学グリーンテクノロジー研究教育センター
バージョン：

Modal Analysis Investigation of Kris Collision Utilizing Finite Element Method

Stesal Waradana[1], Ubaidillah[1,2,*], Aditya Rio Prabowo[1], Bhre Wangsa Lenggana[3], Rahmawati[4], Monsak Pimsarn[5]

[1]Mechanical Engineering, Universitas Sebelas Maret, Surakarta, 57126, Indonesia

[2]Mechanical Engineering, Islamic University of Madinah, Madinah, 42351, Saudi Arabia,

[3]Industrial Engineering, Universitas Jenderal Soedirman, Purwokerto, 53122, Indonesia

[4]Faculty of Economics and Business, Universitas Sebelas Maret, 57126 Surakarta, Indonesia

[5]Mechanical Engineering, King Mongkuts University of Technology Ladkrabang, Bangkok, Thailand

*Author to whom correspondence should be addressed:
E-mail: ubaidillah_ft@staff.uns.ac.id

(Received November 7, 2023: Revised June 8, 2024: Accepted June 21, 2024).

Abstract: Scientific research on krises is still quite limited. Early days of kris, the dissemination of knowledge and technology about kris was done orally through a teacher (empu) and a diligent student who was trusted by the empu. Thus, learning and research on kris is more challenging and makes the secrets of the art of kris more difficult to uncover. In this research, we will study the natural frequency and impact stress of various krises simulated with Ansys software as one of the applications to analyze finite elements. The output of the research is expected that the unique shape of the kris influences the resulting vibration characteristics. The number of Luk variations on the kris affects the natural frequency, stress, and total deformation produced. In the same mode, different results are obtained for each variation of Luk krises, such as in mode 4, Luk 3, Luk 7, and Luk 13 of kris have natural frequency values of 976.73 Hz, 750.78 Hz, and 626.58 Hz, respectively. Thus, the natural frequency, impact stress, and total deformation of each kris variation have different results due to the number of Luk on the kris. The results of total deformation during impact show that the kris variation model's performance also decreases or increases depending on the application.

Keywords: modal analysis; FEM; FEA; kris; finite element

1. Introduction

Countries in the world have a variety of different weapons. The weapons used by the ancient warriors had identities in other forms[1)]. The differences in weapons vary from country to country include weapons in the form of swords and spears. Various variations of shape blades are scattered in different countries in the world because of differences in the function of their use. In addition to functioning weapons, variations shapes of the sword are also used for an artistic function, namely as jewelry. The name used as the identity of a weapon is believed to be just a myth until it is mentioned in literature originating from Europe, which shows that the weapon has a name[1)]. Even prehistoric weapons in the early second half of the first century BC (Before Christ) have found swords with an inscription printed on the blade[2,3)]. This discovery proves that weapons, especially swords, have an identity, namely a name, even since BC. One variation of the shape of the sword is the kris. Besides having beauty, the existence of kris cultural products is also loaded with essential meanings and functions in society that have been used for 600 years. The development of kris weapons has been found in various countries in Southeast Asia, such as Indonesia, Singapore, the Philippines, and Brunei Darussalam. Kris is used as a weapon and a form of the greatness of the king[3)]. Many people believe that the kris has magical powers contained in it. There is still little scientific research involving the kris as the object.

Scientific research on kris is still quite limited. In this research, we will study the natural frequency and impact stress of various types of kris, which will be simulated with Ansys software as an application to analyze finite elements. Finite Element Method (FEM) is a numerical procedure that can be applied to solve various problems in engineering and science[4)]. This method is generally used to solve steady, transient, linear, and nonlinear problems in electromagnetics, structural analysis, and fluid dynamics through a discretization process[5,6)]. The advantage of using FEM is that this method can handle all types of geometric shapes and non-homogeneous materials without changing the formulation code on the

computer[5,6]. The FEM has been widely used to determine the vibration characteristics of a complex structure that is given a moving load[7]. The output of this research expected that the unique shape of the kris influences the characteristics of vibration produced, so the reasons behind the unique shape of the kris will be known.

1.1 Definition and History of Kris

Kris is a stabbing weapon developed in Southeast Asia, especially in the Indonesian archipelago. Kris is known in Central and East Java, Rencong in Aceh, Kujang in West Java, and Badik in Sulawesi[8]. Kris has been known since the days of the Hindu Mataram kingdom[9]. In ancient times, the kris was often used as a gift for outstanding soldiers. As time passes, people are finally allowed to own a kris because previously, the kris could only be owned by those in the kingdom[10]. In making kris, the most needed materials are iron and steel. In addition to iron and steel, other materials are often mixed to make a kris so that a motif is produced and has pores. This material is called Pamor[11]. The Pamor that is mixed with iron and steel when making a kris will produce pores on the blade so that it can be used to absorb a poison liquid that makes a kris a dangerous weapon. The krises that developed in Indonesia have many variants. There are at least 380 types of straight kris and 439 types of kris written in the Ensiklopedia Keris by Ki Hudoyo Doyodipuro[11]. The most popular type for curved kris is the Luk 13 kris, with 20 types. Then there is the Luk 3 kris with 12 types and the Luk 7 with 14 types which are variations of the kris quite popular in Indonesia[12].

1.2 State of the Art

The symbolic meaning of the kris is closely related to Javanese culture. In Javanese culture, kris can show different levels of relationship between the king and the people. Unity by the Javanese is called "Kawulo Gusti" meaning humans and God are interconnected[13]. This unity then makes the kris a unique object that symbolizes the existence of God, who occupies a special place in Javanese culture. The kris is divided into two parts: the sheath (Warangka) and the blade. Symbolic meaning two parts of kris are the sheath (Warangka) as a picture of the people and the blade as the picture of the king. So, if two things are connected, it can be interpreted that the sarong and blade have a dependency, like the people and the king who protect each other. The people protect the king, and the king protects the people through his policies behind the scenes[14].

There are two types of kris based on the time the kris was made which is Tangguh kris and Kamardikan kris[15]. In ancient times the position of the palace was a cultural center, so at that time, the palace's position greatly influenced the development of kris in the archipelago. The emergence of a Tangguh kris is one result of the hegemony of the palace. However, along with the development of the era marked by the independence of the Indonesian nation, at the same time, the palace's influence on kris's development also decreased. Kris Tangguh was made before the independence of the Indonesian nation. This kris was an old kris from the Singosari kingdom to the Surakarta and Yogyakarta kingdoms. The characteristic recognized in Tangguh Kris styles are the character, shape, size, and material that tends to melt, then the master as the kris maker is unknown[16].

Kamardikan kris was made after the independence era. The characteristic of this kris is that it has many new creations according to the will of the kris maker. Then the Kamardikan kris also has a clear maker. Kamardikan kris blades have wide varieties and variations that can be divided into three parts, namely kris with a straight blade, kris with luk and kris new creation[17]. First is a kris with a straight blade as shown in Fig. 1 (Bener/Leres) is a variation with a straight kris blade shape. The basic form of this kris is usually a development of an existing straight kris shape by adding or subtracting the elements of the Ricikan. Ricikan krises are the parts or components of a kris, spear, or sword, each of which has a name.

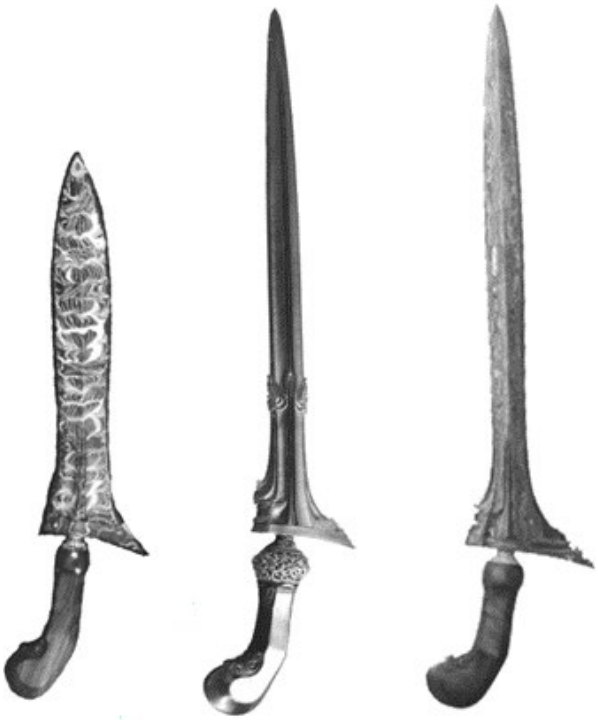

Fig. 1: Straight blade kris

The second is a kris with a blade shape as shown in Fig. 2. Luk's dagger is a variation of a kris with a curved blade shape. Luk is the part of the kris that has a curved shape on the kris. The number of indentations contained in the kris is always odd from Luk 3 to Luk 13. This type of Luk kris will be the object of this study with three types of Luk kris: Luk 3, Luk 7, and Luk 13.

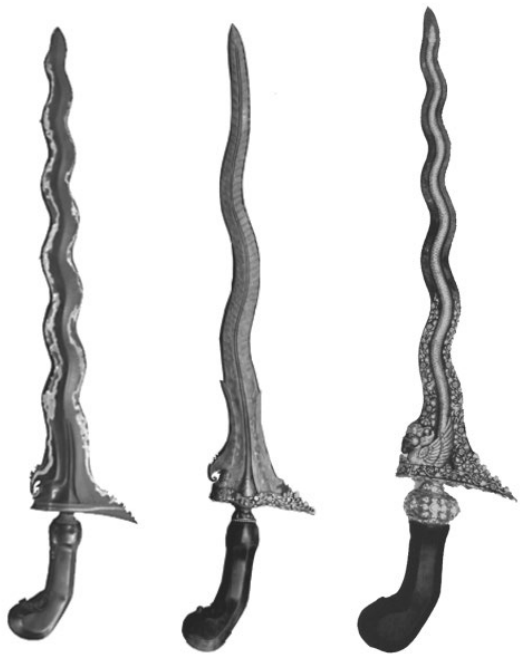

Fig. 2: Kris with Luk

The last is the Luk group based on the new creation kris with a blade variation with a significant shape change compared to the previous kris as shown in Fig. 3. An example of the new creation of kris is the combination of a kris with a Luk shape and a straight shape.

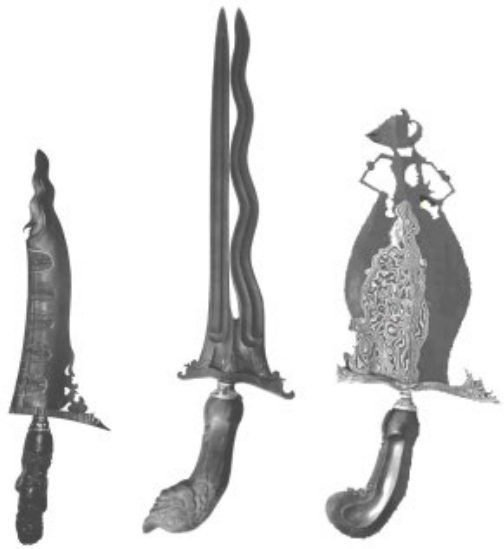

Fig. 3: Kris with the new creation

1.3 Impact and Explicit Dynamics

An impact test is a test using rapid loading. An extensive energy absorption process occurs in the impact test when the load strikes the specimen[18]. Impact testing is carried out to determine the resistance of a material when subjected to sudden loading. Impact testing is also carried out to determine the effects that arise when testing is carried out, such as absorbed energy, stress, and strain to temperature. Impact testing in practice often requires high costs. In order to save high costs, impact testing is first carried out on the simulation software until it is close to the desired material requirements. Then the results are verified through experimental measurements. This study uses explicit dynamics as a tool in the Ansys software to determine the impact stress of the colliding material.

Explicit dynamics is a sub-program of Ansys analysis systems that studies the analysis of transient explicit dynamics that can display simulations of variations in engineering fields, including nonlinear dynamic modeling behavior of solids, fluids, gases, and their related interactions. They are based on explicit methods for solving equations of motion. Explicit dynamics are commonly used in the crash test, drop tests, simulation of forming, pressing, and cutting materials, simulation of gun bullet penetration, and simulation of explosion effect on surrounding structures[19].

1.4 Natural Frequency and Modal Analysis

Understanding the modal response of a system is an essential aspect when evaluating its dynamic characteristics of a solid structure. It is worth emphasizing that modal analysis does not directly calculate the stress and strain within the structure. Rather, its primary focus lies in identifying vibrational attributes like natural frequencies and mode shapes. This analytical approach serves multiple purposes, including the identification and mitigation of resonance frequencies in the system, which is critical for preventing structural failures. Furthermore, it offers valuable insights into how the design reacts under various dynamic loads, aiding in refining and optimizing the structure's performance and durability. Free, undamped vibration is generally governed by a linear equation. This equation describes the object's displacement, velocity, acceleration, and time. In this sense, "free" means the vibration happens without external influences, while "undamped" means there is no friction or air resistance impeding the motion. The mathematical description (Eq. 1) shows how the item travels over time, permitting us to forecast its oscillatory behavior and future positions.

$$[M]\ddot{u} + [K]u = \{0\} \quad (1)$$

where, the mass matrix as well as stiffness matrix are annotated by [M] and [K], respectively. By taking assumption of harmonic motion, the governing equation for eigenvalue can be stated as the following equation (Eq. 2):

$$([K] - \omega_i^2[M])\{\varphi\}_i = \{0\} \quad (2)$$

Eq. 2 can be managed by considering no vibration situation or well-known with trivial solution approach or $\{\varphi\}_i = \{0\}$. Meanwhile, the non-trivial solution can be determined by establishing the zero quantity of eigenvalue equation. The problem can then be resolved for *n* number of degree of freedom $(\omega_1, \omega_2, \omega_3, \omega_4, \ldots . \omega_n)$. The

determined roots are the eigenvalues of the stated equation. Besides eigenvalues, there are corresponding eigenvectors annotated by $\{\varphi\}_1, \{\varphi\}_2, \{\varphi\}_3, \{\varphi\}_4, \ldots . \{\varphi\}_n$. These eigenvectors are considered to be the structural mode shapes as well as its number of mode shape. The eigenvalues can be turned into natural frequencies f_i in Hz following Eq. 3 below:

$$f_i = \frac{\omega_i}{2\pi} \quad (3)$$

In this care, natural frequency of the kris is the primary resonance mode of kris vibration in a system or can also be interpreted as the frequency of vibration caused by disturbances in the form of small impact loads to the kris within a certain period[20,21]. Natural frequency is an essential parameter in representing the dynamic response of the object being tested[22]. Understanding the natural frequency value helps compare how different kris designs vibrate. This comparison helps identify the best shape to minimize vibration when using the weapon, making it more accurate and less likely to miss the target[23]. Modal analysis is an essential technique to help determine the natural frequency as a form of mode in a structure. Modal analysis is used to study the dynamic characteristics of a structure under the influence of vibration[24]. Modal analysis is often used to abstract the modal parameters of a system, including the natural frequency, mode shape, and modal damping[22]. By doing experimental modal analysis (EMA), a structure's natural frequency, mode shape, and damping value can be known. Modal analysis is based on several basic equations of a geometric problem picture that can be seen in the Fig. 4.

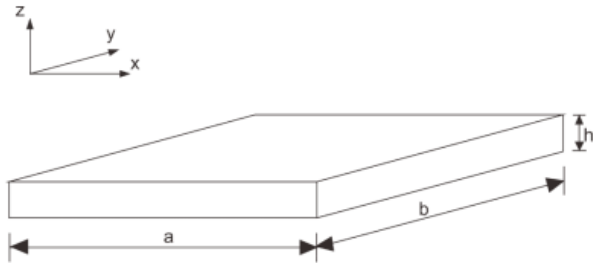

Fig. 4: Thin plate sketch geometry[22]

Based on the figure shown in Fig. 4 above, the plate geometry has infinite degrees of freedom because the determination of the location of each particle on the plate body has infinite coordinates. In this case, it can be assumed that the deflection and linearity have a small value so that the flexural motion equation of the plate can be written as follows (Eq. 4):

$$D = \frac{Eh^3}{12(1-v^2)} \frac{Eh^3}{12(1-v^2)} \quad (4)$$

D is the bending motion; h is plate thickness, E is Young's modulus, and v is Poisson's ratio. In this case, the boundary conditions determine the magnitude of the natural frequency. In contrast, the initial conditions determine the contribution of each mode based on the vibration experienced by the plate. To calculate the natural frequency can use several methods. The first method is to use the Rayleigh method (Eq. 5),

$$\omega^2 = \frac{V_{max}}{\frac{1}{2}hp\iint \emptyset(x,y)dxdy} \quad (5)$$

V_{max} is the maximum speed, $\emptyset(x,y)$ is the boundary condition function of the plate. The second method is the Rayleigh-Ritz method which then writes the formula with the natural frequency in the form ω_n. The Rayleigh-Ritz equation is as follows (Eq. 6),

$$\omega_n = \frac{\lambda_n}{a^2}\sqrt{\frac{D}{\rho h}} \quad (6)$$

where ω_n is the natural frequency, λ_n is the frequency parameter. The third method is the FEM (Finite Element Method) in finding natural frequencies.

1.5 Materials response

Each material under external loading conditions has a different response due to its type and microstructure. In the manufacturing industry, material selection is an essential step so that the material has the right and real properties according to the desired needs. By using FEM, the response of a material can be analyzed. Several material responses to external loadings, such as stress and strain. The stress in a structural member is the internal force divided by the cross-sectional area over which the element acts[25]. To find the stress, Eq. 7 can be used to determine the stress values:

$$\sigma = \frac{F}{A} \quad (7)$$

where F is the normal force, σ is the normal stress, and A is the cross-sectional area. Meanwhile, the strain is a measure of deformation that occurs when stress is generated, Eq. 8 can be used to calculate the strain response:

$$e = \frac{\Delta l}{l_0} \quad (8)$$

where e is the strain, Δl is the increase in length, and l_0 is the initial length.

2. Materials and Methods

2.1 Simulation Setup

The research process commenced with the validation of data from prior studies. This validation involved creating accurate models, replicating the methodology used by Lenggana et al., utilizing SolidWorks for modeling and ANSYS for simulation purposes. The aim of the data validation was to contrast the natural frequency results from previous simulations with those from current

simulations. Upon completion of the new simulations, it was determined that they showed a deviation of less than 5% relative to the findings reported by Lenggana et al[22]. Data validation in the form of previous research experiments was also carried out. The study used as validation is an experiment to the sword. This is done because there is no research both simulation or experimental research in the kris. In previous research three types of swords were conducted, namely a long German sword with a length of 46.38 inches, a Spanish sword with a length of 30.33 inches and a Japanese katana sword with a length of 40.87 inches to compare the simulation results with experimental results. The selection of swords was chosen based on morphological differences, origin of place and availability. In this case, the previous research was used as a validation of the kris study. The results are shown in Table 1. Following the data validation and the determination of the resulting deviation, the subsequent phase involved gathering data using a kris design that included dimensions. The research then proceeded to obtain natural frequency data from the kris, which featured three different Luk variations: Luk 3, Luk 7, and Luk 13. The simulations produced data on natural frequency and amplitude. The models and dimensions of the various Luk modifications to the kris are depicted in Figs 5 to 7, with the dimensions of the model expressed in millimeters for length.

Table 1. Comparison of natural frequency results from experiments and simulations[23]

Mode	German long sword (Hertz)		Spanish sword (Hertz)	
	Experiment	FEA	Experiment	FEA
1	17.1	12.34	23.61	34.56
2	35.06	42.51	59.60	104.47
3	69.84	91.28	117.03	262.00

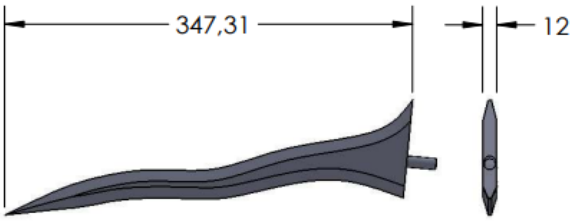

Fig. 5: Luk 3 kris variation

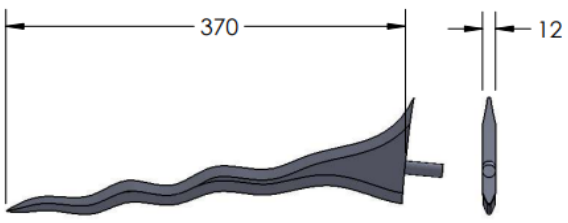

Fig. 6: Luk 7 kris variation

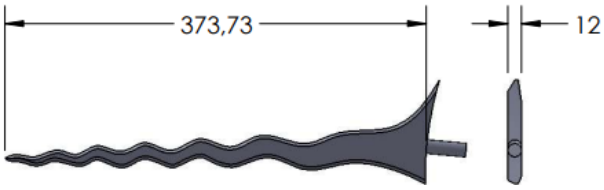

Fig. 7: Luk 13 kris variation

The difference in kris length is due to adjustment to the mass of kris, which must be the same as the three variations of the kris. The mass of the variation of each kris can be seen in Table 2.

Table 2. Mass of each variation of kris

Type of Kris	Mass of Kris
Kris Luk 3	0,69 kg
Kris Luk 7	0,69 kg
Kris Luk 13	0,68 kg

2.2 Materials

The material used is AISI 1095 Carbon Steel. AISI 1095 is high carbon steel famous for use in knives and a wide variety of weapons. One weapon that uses AISI 1095 material is the Katana[26]. AISI 1095 material is used because there has limited research stydy on kris to determine the properties of the material. The materials used in the variations of the Luk 3, Luk 7, and Luk 13 are the same, using AISI 1095 as shown in the following Table 3.

Table 3. Property Material AISI 1095[27]

Properties	AISI 1095 *Carbon Steel*	Unit
Tensile strength, ultimate	525	MPa
Tensile strength, yield	685	MPa
Modulus elasticity	190	Gpa
Poisson's ratio	0.27	-
Shear modulus	80	GPa
Density	7.85	g/cc

2.3 Meshing

Meshing, a crucial step in the FEM, divides a three-dimensional (3-D) object into numerous smaller entities, which allows for a detailed representation of the object's physical form. During the meshing process, defining a smaller or specified mesh size enhances the accuracy of the modeled object. In this specific simulation, face sizing is employed with the finest resolution being a size of 7, as

shown in Fig. 8. Utilizing a fine mesh size is anticipated to augment the precision of the simulation results, bringing them closer to reality.

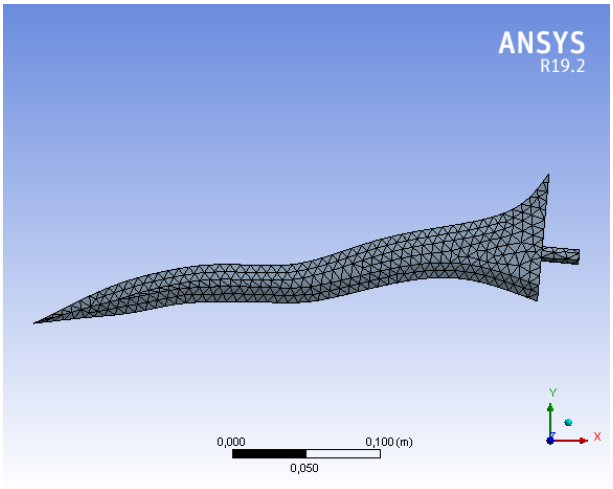

Fig. 8: Meshing process

2.4 Boundary Conditions

The shape of the mode is the number of modes to determine the change in the object's shape being simulated. For this research, 20 Shape Modes will be investigated, but only a few modes will be used as research data. Fixed support provides fixation on selected geometric parts, such as on the surface of an object. Fixed support also provides restraint on the selected part to decrease the degrees of freedom on the selected part. Figure 9 shows the location of the fixed support for the object to be simulated.

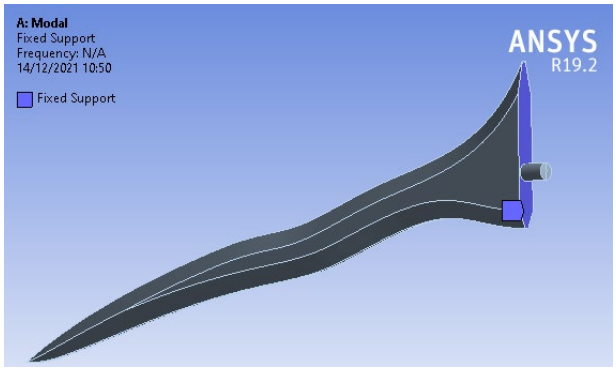

Fig. 9: Fixed support definition

In explicit dynamics, an impact test is carried out with an initial speed set of 10600 mm/s with a force of 175 N during on-top impact or slashing motion and 84000 mm/s with a force of 1885 N during a front collision or stabbing motion[30]. The collision stop time is set to 0.002 s so that the impactor can collide perfectly. The kris collision model can be seen in Fig. 10 and 11 Kris

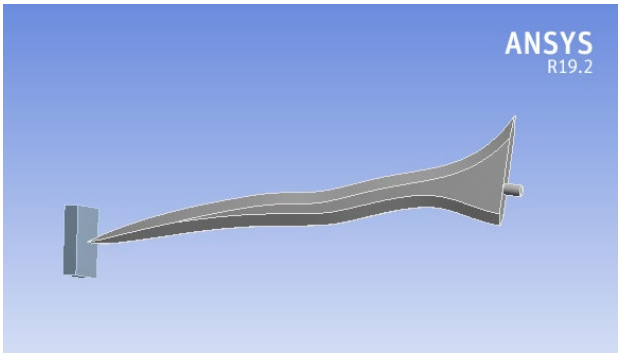

Fig. 10: Front impact

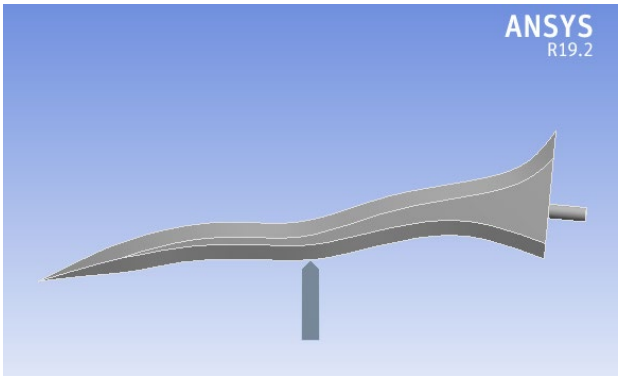

Fig. 11: Side impact

2.5 Result Parameter

After carrying out the data collection process in the form of natural frequencies and impact stresses, the study continued with data analysis by comparing the simulation data of each Luk form so that the best form of kris used as a weapon would be known. Furthermore, conclusions can be drawn from the research that has been done.

3. Result and Discussion

3.1 Natural Frequency

The natural frequency of the three variations of the kris was obtained through modal analysis in Ansys. Modal analysis is needed to help in determining the vibration characteristics, namely the natural frequency and the results of the contour mode shapes of a mechanical structure or component when given dynamic loading. Natural frequency is the oscillation frequency possessed by a system where the vibration by this system is left without additional dampers. Additionally, natural frequency is strongly influenced by the mass and stiffness of a structure. Because mass is an essential factor in determining the value of the natural frequency, in this simulation, the mass of each variation of kris is designed with the same mass. The stiffness of the three variations of kris is equalized by embedding the type of material in all variations of kris.

The modeling of the three variations of the kris has different blade lengths to equalize the kris's mass. The

different shapes of the kris make equating the mass of variations of the three types of kris challenging to achieve. This laborious process is forced to produce a different mass on each kris. The mass difference between the three kris variations does not reach 2% that can be seen in Table 1 above. The natural frequency values of the three variations of the kris can be seen in Fig. 12. Figure 12 shows that there are differences in the natural frequency results of the three variations of the kris. Kris with Luk 3 variation always has the most significant natural frequency value in each mode. The natural frequency value of the Luk 3 kris, which always produces the most outstanding results in all modes, is due to the dimensions of the Luk 3 kris, which have a shorter length than other variations of the kris. This result is under the theory that the longer the blade will reduce the natural value of the resulting frequency[31].

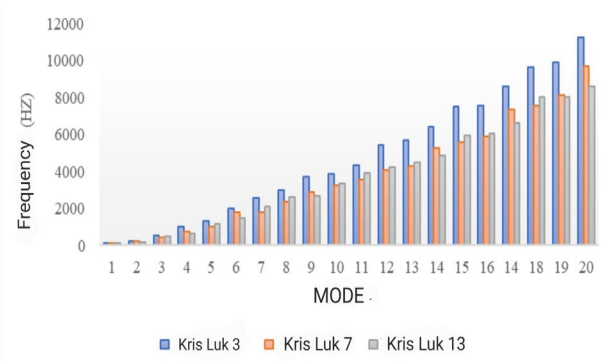

Fig. 12: Comparison curve of natural frequencies between 3 types of Kris variations

For example, the difference in the order of magnitude of the natural frequency value of each variation of the kris can be seen in mode 4 and mode 16 where in mode 4, luk 7 has a higher value than luk 13 while in mode 16, luk 13 has a higher value than luk 7. Table 4 shows the contours of the total deformation of modes 4 and 16 at the variations of the Luk 7 and Luk 13. In mode 4, the Luk kris 3 has a natural frequency value of 976.73 Hz, the Luk 7 kris has a natural frequency value of 750.78 Hz, and the Luk 13 kris has a natural frequency value of 626.58 Hz. The kris with Luk 3 variation has an enormous natural frequency value, than the Luk 7 and Luk 13. In mode 16, the Luk 3, Luk 7, and Luk 13 kris have natural frequency values of 7508.7 Hz, 5881.7 Hz, and 6013.3 Hz, respectively. For mode 16, the enormous natural frequency value was achieved by Luk 3, then the Luk 13 and Luk 7 krisses. There is a difference in the order of the natural frequency values in mode 3 and mode 16, where in mode 3, the Luk 7 kris has the second largest natural frequency value, while in mode 16, the second largest natural frequency value was achieved by the Luk 13 kris then Kris Luk 3 has the greatest value in all modes. To see more clearly the cause of the higher Luk 13 variation value in some modes compared to Luk 7, contour samples will be taken in mode 4 and mode 16.

In Table 4, in mode 4, the variations of Luk 7 and Luk 13 have the maximum total deformation located at the tip of the kris. However, in mode 16, there is the difference in the location of the maximum point for total deformation value, where the kris with a variation of Luk 7 has the maximum value at the tip of the kris, while a variation of Luk 13 is at base of kris. The natural frequency value of Kris Luk 13 in mode 4 reaches 626.58 Hz, and Kris Luk 7 reaches 750.78 Hz. While in mode 16, the natural frequency value produced by the Luk 13 kris reaches 6013.3 Hz and the Luk 6 kris reaches 5881.7 Hz. The difference in contours in modes 4 and 16 causes the order of the natural frequency values of the two modes to be different.

Table 4. Contours of total deformation of mode 4 and mode 16 at variations of Luk 7 and 1

Variation	Mode	
	4	16
Luk 7	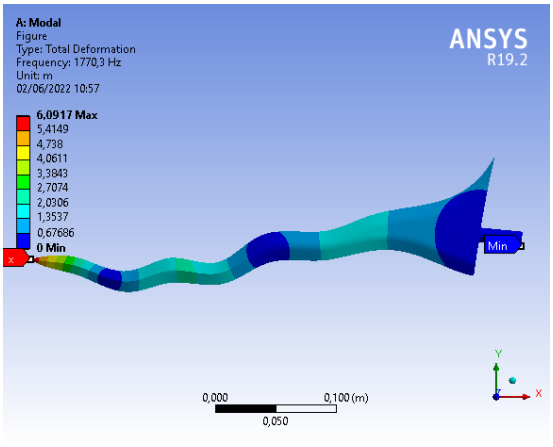	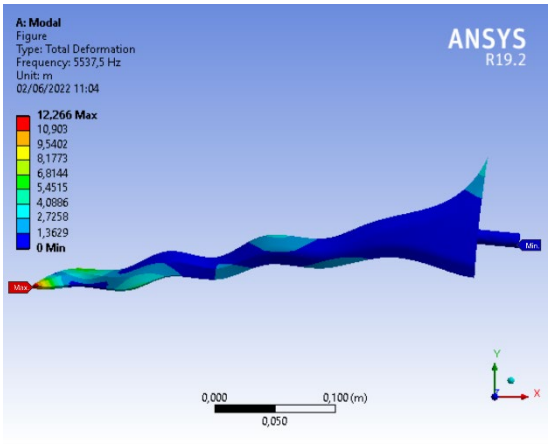
Luk 13	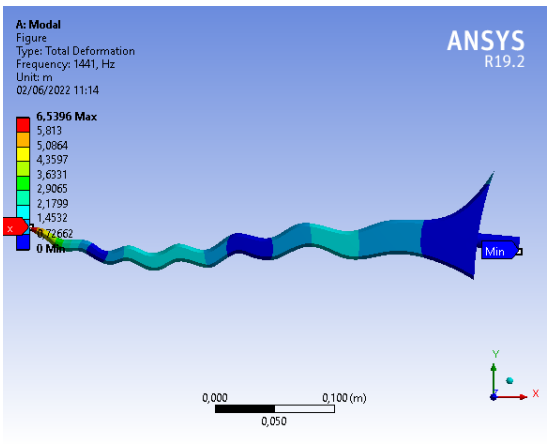	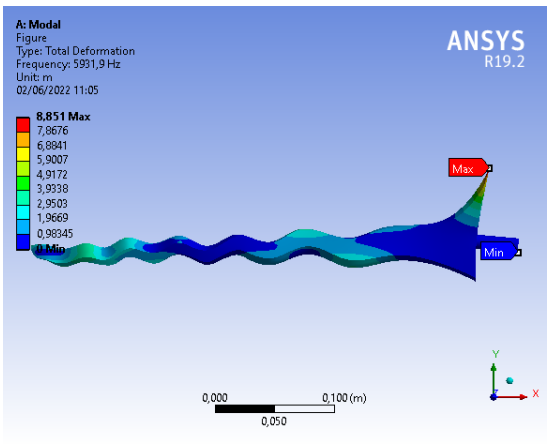

3.2 Von Misses Stress at Front Impact

The collision simulation used explicit dynamics contained in the Ansys software. Explicit dynamics is a sub-program that displays variation simulations in various engineering fields, including nonlinear dynamic modeling such as solid, liquid, gas, and interactions between various types of objects. By using Ansys Explicit Dynamic, a model's physical visualization can be done quickly[32-34]. This simulation modeling describes how the stabbing motion. This simulation is run with the movement of kris on the X axis, which will hit the impactor with a speed of 8.4 m/s and a peak force of 1885 N[29] where the setting is obtained from research that observes response of knife when a stabbing motion is carried out on the armor.

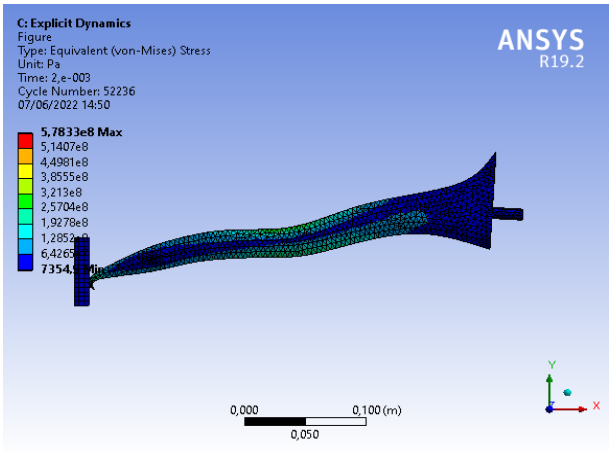

Fig. 13: von misses stress of Luk 3 front impact

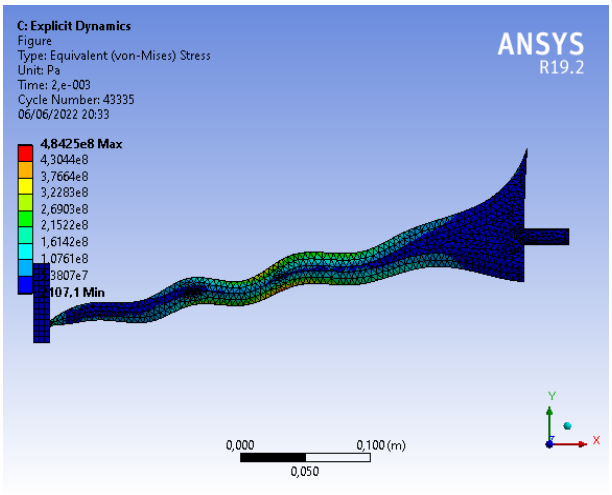

Fig. 14: von misses stress Luk 7 front impact

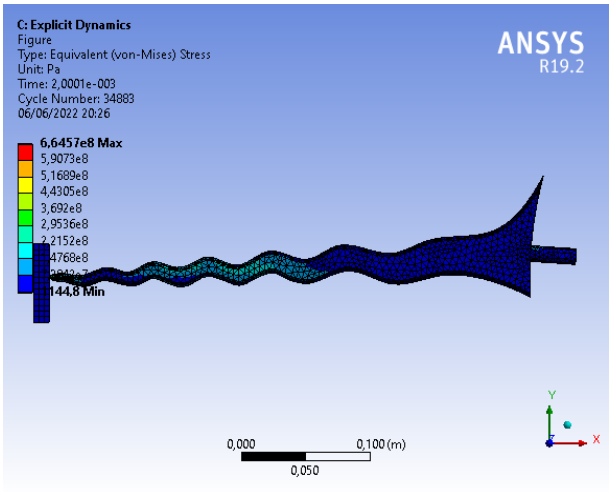

Fig. 15: von misses stress Luk 13 front impact

The contour depictions of the simulation results for the front impact with the stabbing motion are shown in Fig. 13, 14, and 15. These images show the differences in the stress and contour results in the three variations of the simulated kris. The enormous von misses stress is produced by the Luk 13 kris with a size of 664 MPa, then the Luk 3 kris with a size of 578 MPa, and the smallest is the Luk 7 kris with a size of 484 MPa. Based on the contour color generated in the simulation, it can be observed on all types of kris that the most significant stress is generated when the kris strikes the impactor at the tip of the kris. While the stress distribution is based on the color of the contour, the kris with the variation of Luk 3 is spread on the second curve than on the kris with the variation of Luk 7 on the fifth curve and Luk 13 on the seventh curve. This can happen because of the difference in the number of indentations by each shape of the kris. The most extensive contour distribution describes the breadth of the stress distribution that occurs on the kris and is marked with a yellow color which tends to be in the middle of the kris, so it causes differences in the distribution location based on the curve of the kris. The most significant stress produced by kris with a variation of Luk 13 is caused by the shape of the kris, which tends to be straight with the impactor. From Fig. 13, and Fig.14 can be seen the kris with the Luk 3 variation has a higher maximum tension than the Luk 7 variation because it has a straighter shape with the impactor, so it has a smaller collision angle.

From the front impact simulation that has been carried out, data is obtained in the form of an average von misses stress compared to time with an end time setting of 0.002 s from variations of the Luk 3, 7, and 13 krises. The simulation data comparison curve is an average von misses stress compared to the time of variations of the Luk 3, Luk 7, and Luk 13 can be shown in Fig. 16.

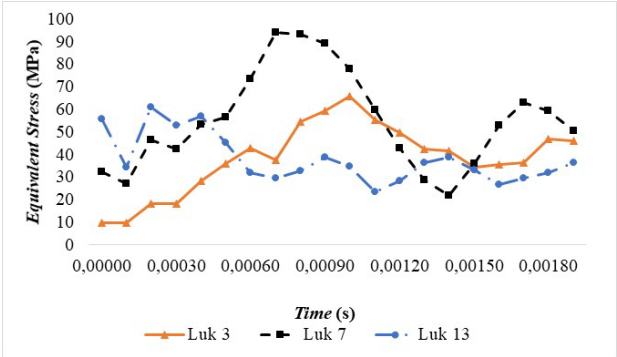

Fig. 16: Comparison curve of von misses stress versus time between 3 types of kris variation

The rapid onset of impact stress, occurring within a fraction of a millisecond, is a critical aspect influencing the observed results. The presence of a discernible peak on the stress-time graph in Fig. 16 signifies the occurrence of impact or collision, indicating the moment when the dagger makes contact with the impactor. Notably, the kris variation with Luk 7 exhibits the most prominent peak stress, averaging at 93.7 MPa. However, this variation also demonstrates substantial stress levels at the end time, suggesting a persistence of stress beyond the initial impact phase. Conversely, the kris with Luk 3 variation displays peak stress and stress levels at the end time that are the second highest among the kris variations studied. This indicates a significant stress response to impact, albeit slightly lower than that of the Luk 7 variation. In contrast, the Luk 13 variation exhibits the lowest peak stress and stress levels at the end time. This observation suggests that the Luk 13 configuration may offer superior stress dissipation or absorption capabilities, resulting in reduced stress magnitudes both at the point of impact and over time. Overall, these results underscore the complex interplay between impact dynamics, kris configuration, and stress response, highlighting the importance of considering these factors in the design and optimization of dagger structures for enhanced performance and durability.

3.3 Von Misses stress at side impact

This simulation model illustrates how the slashing motion is. This simulation is run with the movement of the kris on the Y axis, which will hit the impactor with a speed of 10.4 m/s and with a peak force of 175 N obtained from research on the slashing motion of a knife worn on a Kevlar shirt[29,35,36]. The impact is in the middle of the number of indentations possessed by each shape of the kris. Imposition on the middle of the number of Luk kris is done because if it is applied right in the middle of the dimensions of the kris, then the collision will hit a different part of the curve of each kris resulting in a different reaction as well as shown in Fig. 17, 18 and 19.

The contour plots presented in Fig. 17, 18, and 19 offer a detailed visual representation of the stress distribution resulting from side impact simulations across the three variations of the kris. These figures highlight distinct differences in stress patterns and contours among the simulated kris variations subjected to side collisions. Remarkably, the stress distribution observed in the side impact simulations mirrors the sequence observed in the front impact simulations, with consistent order from highest to lowest stress levels. Specifically, the Luk 13 kris exhibits the highest von Mises stress, measuring at 553 MPa, followed by the Luk 3 kris at 525 MPa, and finally, the Luk 7 kris displaying the lowest stress magnitude at 469 MPa. Analyzing the contour distribution of stress results across kris variations, it becomes evident that stress is predominantly concentrated in the collision area initially, subsequently spreading to regions with smaller cross-sections, particularly towards the tip of the kris. This stress distribution pattern suggests that the kris variations respond differently to the lateral forces exerted during side impacts, with stress propagating from the point of impact towards areas with lesser structural reinforcement.

Furthermore, the data gleaned from the side impact simulations provides valuable insights into the temporal evolution of stress distribution. By setting an end time of 0.002 s, the simulations enable the comparison of average von Mises stress over time across the Luk 3, 7, and 13 kris variations. This temporal analysis offers a comprehensive understanding of how stress levels evolve throughout the duration of the impact event, shedding light on the dynamic response of each kris variation to lateral forces. In essence, the combination of contour plots and temporal stress data from the side impact simulations enhances our understanding of how different Luk variations influence stress distribution and response characteristics during lateral collisions, providing crucial information for optimizing kris design and structural integrity. The timing of the variations of the Luk 3, Luk 7, and Luk 13 kris can be shown in Fig. 20.

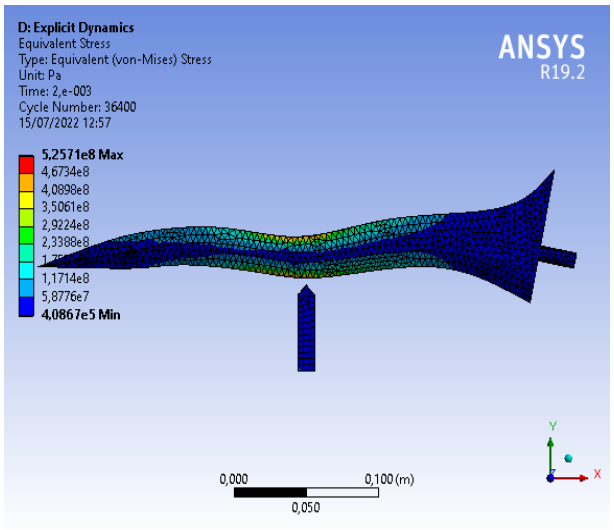

Fig. 17: von misses stress Luk 3 side impact

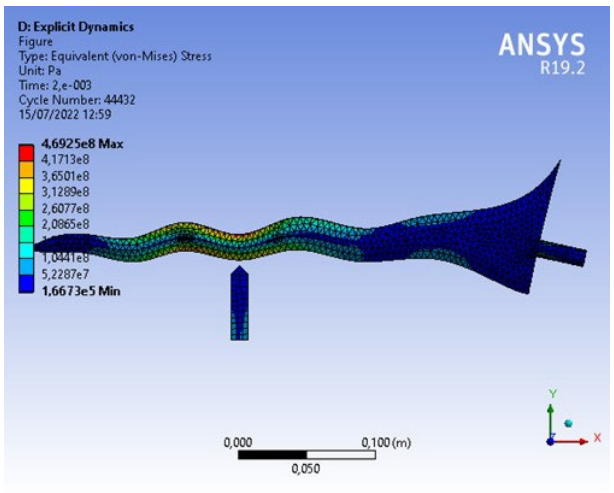

Fig. 18: von misses Luk 7 side impact

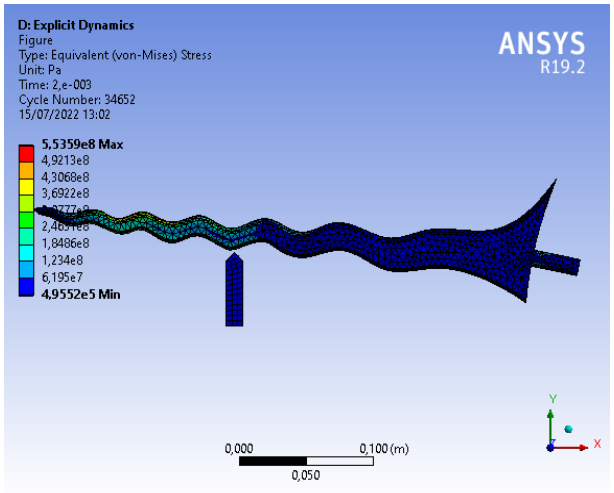

Fig. 19: von misses Luk 13 side impact

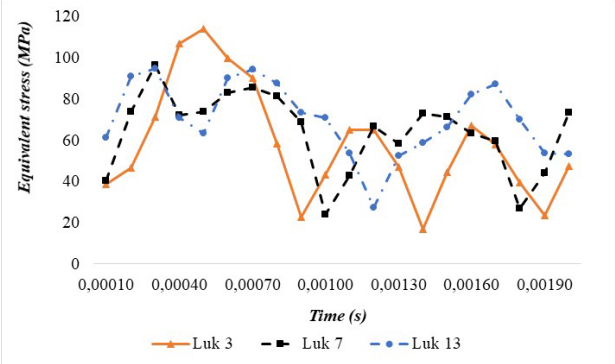

Fig. 20: Comparison curve of von misses stress versus time between 3 types of kris variation

The variation in stress distribution observed in Fig. 20 can be attributed to several factors. Firstly, the kris with Luk 3 variation exhibits the highest peak stress of 114 MPa immediately after the collision. This can be attributed to the specific configuration of Luk 3, which may concentrate stress at certain points upon impact due to its placement and geometric characteristics. However, despite initially experiencing the highest stress, the Luk 3 variation demonstrates a relatively efficient stress reduction mechanism over time, maintaining the second-largest stress value until the end time. This suggests that while the Luk 3 variation may initially concentrate stress, its overall structural integrity and stress distribution mechanisms effectively dissipate stress over time. Conversely, the Luk 7 variation displays the second-highest peak stress of 96 MPa, indicating a slightly lower stress concentration compared to Luk 3 immediately after the collision. However, as the simulation progresses, the Luk 7 kris exhibits a significant increase in stress, culminating in an enormous stress value by the end time. This phenomenon suggests that while the Luk 7 variation initially distributes stress relatively evenly, its structural characteristics may lead to stress accumulation or ineffective stress dissipation mechanisms over time, resulting in a substantial increase in stress. On the other hand, the Luk 13 variation demonstrates the lowest peak stress of 94 MPa immediately after the collision. This indicates that the Luk 13 configuration may effectively disperse stress upon impact, resulting in lower localized stress concentrations compared to Luk 3 and Luk 7. However, similar to Luk 7, the Luk 13 kris experiences a notable increase in stress over time, ultimately reaching the second-highest stress value at the end time. This suggests that while the Luk 13 variation initially distributes stress effectively, it may encounter limitations in stress dissipation mechanisms or structural stability over the duration of the simulation.

3.4 Total Deformation

In addition, this study will not only compare the stress levels in three different kris variations but will also analyze additional research data on total deformation to support the findings. Total deformation is an option in the Ansys function to observe the simulated object's deformation results in three coordinates X, Y, and Z as shown in Fig. 21.

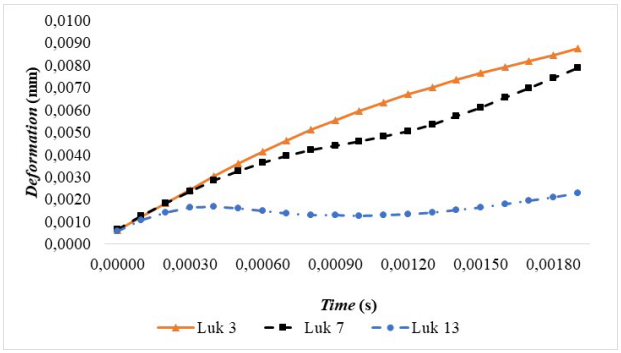

Fig. 21: Average total deformation of front impact simulation

The curve trend in Fig. 21 shows that the Luk variation affects the total deformation value produced during the forward collision or stabbing motion. During the start time at t=0 s, the variations of the Luk 3, Luk 7, and Luk 13 showed deformations of 6.04 x 10-3 mm, 6.5 x 10-3 mm, and 5.9 x 10-3 mm, respectively. Meanwhile, at the end of time, the Luk 3, Luk7, and Luk 13 kris showed deformation of 8.74 x 10-3 mm, 7.88 x 10-3 mm, and 2.27 x 10-3 mm, respectively. The curve shows that the enormous total deformation value is produced by the Luk 13, then Luk 7, and Luk 3, respectively. Figure 21 also shows that the greater the number of Luk variations on the kris, the smaller the total deformation produced. Increasing the number of luk (waves or curves) on a Kris distributes stress more evenly along its length. When force is applied to the dagger, whether through impact or pressure, the waves act as points of stress dispersion. This means that the force applied to the Kris is less concentrated in any one area, reducing the likelihood of deformation or structural failure. The more luk a Kris has, the more rigid it becomes. This increased rigidity helps the Kris resist bending or warping when subjected to external forces. Think of it like adding additional reinforcement to a structure; each luk adds strength and stability to the overall design.

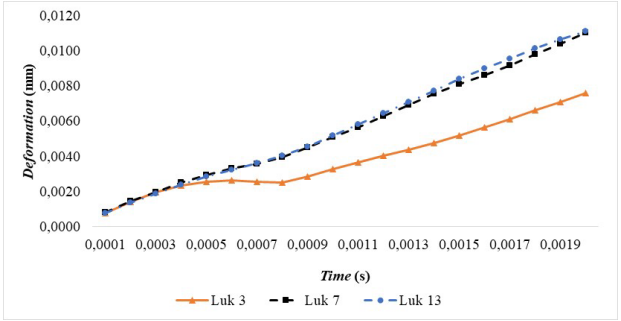

Fig. 22: Average total deformation of side impact simulation

The curve's trend in Fig. 22 shows that the variation of Luk affects the total deformation value produced during the top collision or slashing motion. During the starting time, the variations of the Luk 3, Luk 7, and Luk 13 krises showed deformations of 7.54 x 10-3 mm, 8.29 x 10-3 mm, and 7.56 x 10-3 mm, respectively. Meanwhile, at the ends of the kris, the deformation is 7.59 x 10-2 mm, 11.01 x 10-2 mm, and 11.10 x 10-2 mm. The curve shows that the enormous total deformation value is produced by the Luk 13, then Luk 7 and Luk 3 krises, respect ively. Figure 22 also shows that the more Luk variations on the kris, the greater the total deformation produced. Luk act as stress concentrators, redistributing stress throughout the kris structure. When more luk are present, the stress is more evenly distributed across the kris, reducing localized stress concentrations that can lead to deformation.

4. Conclusion

Simulation studies using the FEM method with Ansys software have been carried out by varying the number of Luk on the kris. From this work, it can be concluded that the number of variations of Luk on the kris influences the natural frequency, stress, and total deformation produced. In the natural value, the frequency of the kris with the variation of Luk 3 has an enormous value in each mode because it has the shortest dimension compared to other variations of the kris. The difference in natural frequency values for the Luk 3 kris variation is 24.07% higher than the Luk 7 and Luk 7 kris 0.80% higher than the Luk 13 kris. The total deformation value with the forward collision simulation shows that the more variations in the number of Luk, the smaller the resulting value. The Luk 13 kris has the highest total deformation value with an average difference of 0.24% higher than the Luk 7 kris. Then the Luk 3 kris has the lowest total deformation value with a 39.82% difference lower than the Luk 7 kris. Meanwhile, the total deformation value during side collisions shows that the greater the number of Luk variations, the greater the total deformation value. The Luk 3 kris has an average difference in the total deformation value of 16.35% compared to the Luk 7 kris. Then the Luk 13 kris has the lowest total deformation value with a difference of 186.38% lower than the Luk 7 kris. There are several trends visible in this study. Based on the impact received from the front, a greater number of luks tends to have a lower deformation effect. Meanwhile, for side impact results, a larger number of luks tends to increase the deformation value. So for impact loads from the front, luk 13 is better than the other variations, while impact from the side, on the other hand, luk 3 is better than the other variations. The impact stress resulting from the variation of the kris has the same order based on its most significant value when there is a front or side collision. A kris with a variation of Luk 13 has the most significant stress value than Luk 7 and Luk 3, respectively. At the time of the front collision, the most significant stress value was produced by the Luk 13 kris with 664 MPa, which has a difference of 14.88% compared to the Luk 7 kris. At the time of side collision, the most significant stress value produced by the Luk 13 kris with 553 MPa has a difference of 5.33% greater than the Luk 3 kris. In comparison, the Luk 7 kris produced the smallest value produced during the front collision with 484 MPa, which is 19.42% smaller than the Luk 3 kris. The slightest stress value produced by the Luk 7 kris during the side collision was 469 MPa, with a difference of 11.94% lower than the Luk 3 kris. The stress distribution patterns observed in this study reflect the complex interplay between the geometric characteristics of Luk variations, stress concentration mechanisms, and stress dissipation mechanisms over time. While each Luk variation demonstrates unique stress response characteristics, further analysis is required to understand the underlying structural factors influencing stress distribution and dissipation in greater detail.

Acknowledgements

This research was funded by Kementerian Pendidikan, Kebudayaan, Riset, dan Teknologi (Kemdikbudristek) Republik Indonesia under Hibah Penelitian Terapan 2024.

References

1) M. Pearce, "The spirit of the sword and spear," Cambridge Archaeological Journal, vol. 23, no. 1, pp. 55–67, Feb. 2013, doi: 10.1017/S0959774313000048.
2) R. Wyss, "The Sword of Korisios," Antiquity, vol. 30, no. 117, pp. 27–28, 1956, doi: 10.1017/S0003598X00026399.
3) E. Sedyawati, “Keris Pada Masa Jawa Kuna,” in Keris dalam perspektif keilmuan, Pusat Penelitian dan Pengembangan Kebudayaan, Badan Pengembangan Sumber Daya Kebudayaan dan Pariwisata, Kementerian Kebudayaan dan Pariwisata, Republik Indonesia, 2011, pp. 27–32.
4) T. Yuwono, “Keris Sebagai Kajian Objek,” in Keris dalam perspektif keilmuan, Pusat Penelitian dan Pengembangan Kebudayaan, Badan Pengembangan Sumber Daya Kebudayaan dan Pariwisata, Kementerian Kebudayaan dan Pariwisata, Republik Indonesia, 2011, pp. 145–184.
5) S. S. Law, J. Q. Bu, X. Q. Zhu, and S. L. Chan, "Moving load identification on a simply supported orthotropic plate," International Journal of Mechanical Sciences, vol. 49, no. 11, pp. 1262–1275, Nov. 2007, doi: 10.1016/j.ijmecsci.2007.03.005.
6) T. H. T. Chan and D. B. Ashebo, "Theoretical study of moving force identification on continuous bridges," Journal of Sound and Vibration, vol. 295, no. 3–5, pp. 870–883, Aug. 2006, doi: 10.1016/j.jsv.2006.01.059.
7) M. Siswosuwarno, “Teknologi Perkerisan: Kajian Metalurgis,” in Keris dalam perspektif keilmuan,

Pusat Penelitian dan Pengembangan Kebudayaan, Badan Pengembangan Sumber Daya Kebudayaan dan Pariwisata, Kementerian Kebudayaan dan Pariwisata, Republik Indonesia, 2011, pp. 187–197.
8) Mukhsadad Ahmad, “Makna Keris dan Pengaruhnya Terhadap Masyarakat di Surakarta,” 2008.
9) Guntur, “The Pendhok Style of Surakarta Kris a Case Study of Dhoni Kustanto as Pendhokartist of 90s Mranggi Generations,” Surakarta, Oct. 2007. [Online]. Available: http://kesolo.com
10) D. Dharsono, M.Sn, "Kris Nusantara: Kris As a Bond of Socio-Cultural Values Shifts Into Individual-Cultural Bonds and as Asset in Business Alternatives," ARTISTIC : International Journal of Creation and Innovation, vol. 1, no. 1, pp. 38–54, Mar. 2020, doi: 10.33153/artistic.v1i1.3004.
11) Doyodipuro Hudoyo, “Terlahirnya Sebilah Keris,” in KERIS: Daya magic, Manfaat, Tuah Misteri, 9th ed., Semarang: Dahara Prize, 2004, pp. 39–69.
12) Winter F.L Tuan, Kitab Klasik Tentang Keris, 1st ed. Yogyakarta: Panji Pustaka, 2009.
13) N. Siswanto, “Ajaran Moral Keris Jawa,” CORAK, vol. 2, no. 1, May 2013, doi: 10.24821/corak.v2i1.2331.
14) E. Wijayanto, "International Review of Humanities Studies Keris as a Culture Text: Hermeneutics Review of Pusaka Keris Magazine," 2019. [Online]. Available: www.irhs.ui.ac.id,
15) K. Wasi, “Eksistensi Keris Jawa Dalam Kajian Budaya,” Surakarta, 2019.
16) Supriaswoto and T. Haryono, “Pertalian Tradisi Keris Tangguh Yogyakarta: Titik Awal dan Kebangkitan Historis,” Yogyakarta, 2012.
17) Kuntadi Wasi Darmojo, “Keris Kamardikan,” vol. 11, no. 2, pp. 123–137, 2014.
18) Yunus Muhammad, Najamudin, and Kurniadi, “Pengaruh Perlakuan Quenching-Tempering Terhadap Kekuatan Impak Pada Baja Karbon Sedang,” vol. 2, no. 1, Oct. 2016.
19) L. Caban, D. Marasová, and L. Ambriško, "Methodology of the impact process applying the Finite Element Method," TEM Journal, vol. 8, no. 3, pp. 775–781, 2019, doi: 10.18421/TEM83-11.
20) H.-F. Wang, J. Kun-Kun, and G. Zi-Peng, "Random vibration analysis for the chassis frame of hydraulic truck based on ANSYS," Available online www.jocpr.com Journal of Chemical and Pharmaceutical Research, vol. 6, no. 3, pp. 849–852, 2014, [Online]. Available: www.jocpr.com
21) F. Liu and R. Fan, "Experimental Modal Analysis and Random Vibration Simulation of Printed Circuit Board Assembly," 2013.
22) B. W. Lenggana et al., "Effects of mechanical vibration on designed steel-based plate geometries: Behavioral estimation subjected to applied material classes using finite-element method," Curved and Layered Structures, vol. 8, no. 1, pp. 225–240, Jan. 2021, doi: 10.1515/cls-2021-0021.
23) K. Marut and T. Michael, "Unsheathing the Vibrational Dynamics of Swords." [Online]. Available: http://science.howstuffworks.com/sword-making1.htm
24) C. M. Ramesha, A. K. G, A. Singh, A. Raj, C. S. Naik, and A. Professor, "International Journal of Emerging Technology and Advanced Engineering Modal Analysis and Harmonic Response Analysis of a Crankshaft," 2008. [Online]. Available: www.ijetae.com
25) J Macdonald Angus, TextboStructure & Architecture, 2nd Edition. London, 2001.
26) "1095 Carbon Steel Guide - Medieval Swords World." https://medievalswordsworld.com/1095-carbon-steel-guide/ (accessed Jun. 16, 2022).
27) “AISI 1095 Carbon Steel (UNS G10950),” https://www.azom.com/article.aspx?ArticleID=6561 (accessed Jun. 16, 2022)
28) X. Zou, C. Yang, and B. Liu, "The Contact and Transient Dynamic Analysis of Gear Meshing with ANSYS," OALib, vol. 07, no. 09, pp. 1–9, 2020, doi: 10.4236/oalib.1106771.
29) R. Vicente and P. Rezende, "Example of Mesh Generation on ANSYS ICEM Some of the authors of this publication are also working on these related projects: waste water treatment View project Development of Closure Model for Two-Phase Flow View project," 2016, doi: 10.13140/RG.2.1.1050.7121.
30) J. Cavanaugh, C. Bir, and N. Rowley, "Characterization of Weapons used in Stab/Slash Attacks."
31) L. K. Tartibu, M. Kilfoil, and V. der Merwe, "Vibration Analysis Of a Variable Length Blade Wind Turbine," 2012.
32) J. S. Budi, Ubaidillah, A. R. Prabowo, A. Esdiyanto, Z. Arifin, and Z. E. Priyatama, “Numerical Analysis of Bifilar Coil Geometry on Induction Heating Performance for Self-healing Asphalt,” Evergreen: Joint Journal of Novel Carbon Resource Sciences & Green Asia Strategy, 10 (1), 574-584 (2023). doi: 10.5109/6782164.
33) A. Kumar, A. K. Chanda, and S. Angra, " Numerical Modelling of a Composite Sandwich Structure Having Non Metallic Honeycomb Core," Evergreen. Vol. 08 (4), pp759-767 (2021). doi:10.5109/4742119
34) B. Rusdyanto, F. Imaduddin, Ubaidillah, and D. Ariawan, “The Tensile Properties of Recycled Polypropylene Filament (rPP) as 3D Printing Material,” EVERGREEN Joint Journal of Novel Carbon Resource Sciences & Green Asia Strategy, Vol. 10 (1), pp489-495, (2023). doi:10.5109/6782152
35) I. Choirunisa, Ubaidillah, F. Imaduddin, and E. T. Maharani, “MR Damper Modeling using Gaussian and Generalized Bell of ANFIS Algorithm,” Journal of Novel Carbon Resource Sciences & Green Asia

Strategy, Vol. 08 (03), pp673-685, (2021). doi:10.5109/4491844

36) M. Awi and A. S. Abdullah, " A Review on Mechanical Properties and Response of Fibre Metal Laminate under Impact Loading (Experiment)," Evergreen. Vol. 10 (1), pp111-129 (2023). doi:10.5109/6781057